Electronic Supplementary Information

Partial hydrogenation induced interaction in a graphene-SiO_2 interface: Irreversible modulation of device characteristics

[1*]Takuya Iwasaki, [1*]Manoharan Muruganathan, [1]Marek E. Schmidt [1,2,3]Hiroshi Mizuta

Transport Measurements of Monolayer and Bilayer GFETs

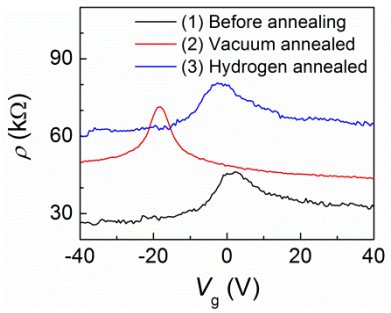

Fig. S1 Resistivity ρ versus back-gate voltage V_g characteristics at 300 K of the monolayer GFET before annealing (black), after vacuum annealing (red), and after hydrogen annealing with the vacuum annealing treatment (blue), respectively.

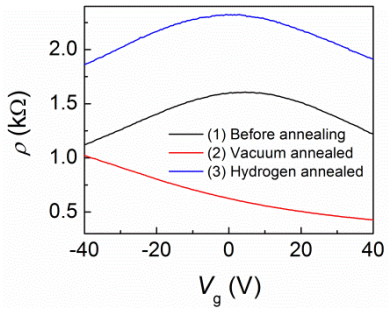

Fig. S2 Resistivity ρ versus back-gate voltage V_g characteristics at 300 K of the bilayer GFET before annealing (black), after vacuum annealing (red), and after hydrogen annealing with the vacuum annealing treatment (blue), respectively.

Figures S1 and S2 show the resistivity (ρ) of the monolayer and bilayer GFETs as a function of back-gate voltage (V_g) measured at room temperature for all experiment steps, respectively. Before annealing, almost GFETs including monolayer and bilayer devices show the charge near CNP in the positive V_g at 300 K. The p-doping effect is caused by physisorbed O_2 and H_2O molecules onto the surface[1,2] or the water layer at the interface between graphene and SiO_2.[1,3] However, some devices randomly exhibit the CNP in the negative side or near 20 V, which might be attributed to unintentional contaminations or impurities. After vacuum annealing, a negative shift of the CNP is observed in the almost GFETs. This result can be ascribed to the removal of p-type dopants from the graphene

surface and the interface of graphene/SiO_2[4] and charge transfer from SiO_2 to graphene.[5] After hydrogen annealing and the vacuum annealing treatment, the CNP is found around V_g ~0 V and the overall resistivity increases as well as the trilayer GFETs. The observation of the CNP close to 0 V indicates that either p- or n-doping level was reduced. According to our DFT calculation, the small shift of the CNP and the irreversible reduction of the overall conductivity can be attributed to a decrease in distance between the graphene and the SiO_2 substrate due to partial hydrogenation at the SiO_2 surface.

DFT Calculations

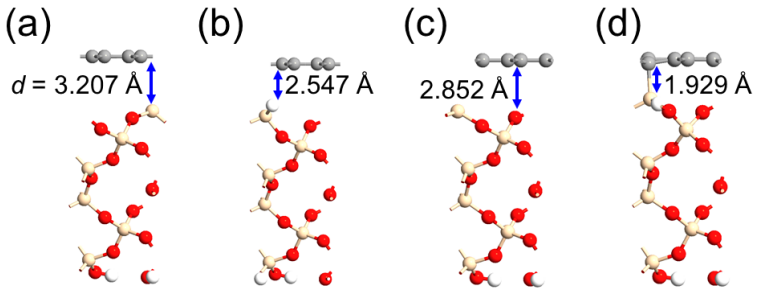

Fig. S3. Atomic configuration side view of the geometrically optimized structure of monolayer graphene on Quartz SiO_2 (0001) surface: (a) without any defects, and (b) one of the silicon dangling bonds in (a) is terminated by a hydrogen with GGA-RPBE exchange correlation functionals with DFT-D3 corrections; (c) without any defects, and (d) one of the silicon dangling bonds in (a) is terminated by a hydrogen with LDA exchange correlation functionals.

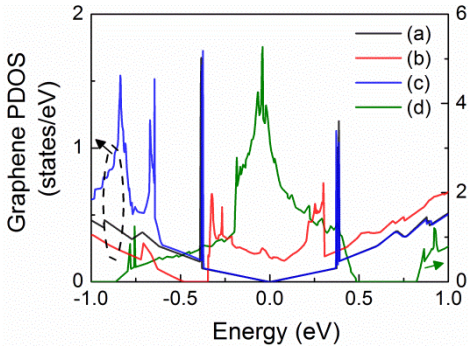

Fig. S4. PDOS plot of the monolayer graphene of the geometrically optimized structures shown in Fig. S3 with exchange correlation functionals of GGA-RPBE with DFT-D3 corrections and LDA.

Monolayer graphene/SiO_2 system simulations were done with and without hydrogenation at the graphene/SiO_2 interface. Details of the simulation method are given in the main text. To analysis the interaction between monolayer graphene and SiO_2 substrate, DFT calculations were done with revised Perdew-Burke-Ernzerhof parametrization of the GGA (GGA-RPBE)[6] functional with the Grimme DFT-D3 dispersion and LDA functional. For DFT-D3 calculation, distance between the graphene and the top SiO_2 surface is 3.207 Å, which is reduced to 2.547 Å

when a single dangling bond of a Si atom is terminated by the hydrogen (Figs. S3(a) and (b)). In the case of For the LDA functional, optimized distance between the graphene and the top of SiO_2 surface is 2.852 Å. This value is lower than interlayer distance of graphite. When a single dangling bond of a Si atom is terminated by the hydrogen then strong Si-C bond is formed with 1.9 Å bond length (Figs. S3(c) and (d)). This leads to a high density of defect states around the Fermi level and the band-gap opening at low and higher energies (Fig. S4(d)).

REFERENCES

1. F. Schedin, A. K. Geim, S. V. Morozov, E. W. Hill, P. Blake, M. I. Katsnelson and K. S. Novoselov, *Nat. Mater.*, 2007, **6**, 652-655.
2. Y. Sato, K. Takai and T. Enoki, *Nano Lett.*, 2011, **11**, 3468-3475.
3. H. Komurasaki, T. Tsukamoto, K. Yamazaki and T. Ogino, *J. Phys. Chem. C*, 2012, **116**, 10084-10089.
4. K. Kumar, Y. S. Kim and E. H. Yang, *Carbon*, 2013, **65**, 35-45.
5. H. E. Romero, N. Shen, P. Joshi, H. R. Gutierrez, S. A. Tadigadapa, J. O. Sofo and P. C. Eklund, *ACS Nano*, 2008, **2**, 2037-2044.
6. Y. Zhang and W. Yang, *Phys. Rev. Lett.*, 1998, **80**, 890.